Assessment of the Geothermal Potential of Fault Zones in Germany by Numerical Modelling

Jörg Kuder

Leibniz-Institute for Applied Geophysics, Stilleweg 2, D-30655 Hannover

joerg.kuder@leibniz-liag.de

Keywords: Geothermal potential, fault zones, Germany, numerical modelling.

ABSTRACT

The shortage of fossil energy sources and the impact of their combustion residues on the environment led to the search of appropriate alternatives. One of them is the use of deep geothermal energy. A successful geothermal power plant needs a productive geological setting. To identify such a setting research was carried out e.g. by Nathenson (1975), Muffler and Cataldi (1978), Economides and Ungemach (1987), Gringarten (1987), Haenel and Staroste (1988), Horne (1988), Jain et al. (2015) and many others. In 2002, the Institut für Geowissenschaftliche Gemeinschaftsaufgaben (GGA, renamed to Leibniz Institute for Applied Geophysics (LIAG) in 2008) and the Federal Institute for Geosciences and Natural Resources (BGR) provided an "Assessment of the technical potential of the geothermal power production and geothermal combined heat and power generation in Germany" (Jung et al. 2002). The investigated geological environments were hot water aquifers, fault zones and crystalline rocks. Fault zones with significantly better permeabilities than the surrounding unfaulted rock can act as natural migration paths for ascending fluids that are able to transport thermal energy from deep geological formations (i.e. Gringarten et al. 1975, Rühaak et al. 2010). If the width of the faults is tens of meters and contain a remarkable amount of water, they store geothermal energy similar to aquifers. Under these circumstances, fault zones are interesting for geothermal utilisation especially those in at least less than 7 km depth.

1. INTRODUCTION

One objective of the joint project "The role of deep rooting fault zones for geothermal energy utilization" supported by the Federal Ministry for Economic Affairs and Energy was the evaluation of the geothermal potential of fault zones in Germany by means of numerical modelling with COMSOL. To achieve this goal a method was developed to estimate the potential of regional generalized fault zones to produce electric power for a lifetime of 50 years with the condition that fluid temperatures are equal or greater than 100 °C. A cube with 1 km side length serves as unified numerical model including a 20 or 50 meter broad, 1000 m high and 1000 m long fault zone (Fig. 2). The numerical models were calculated with a variety of fluid and rock property parameters for four representative regions in Germany and depth ranges of 3-4 km, 4-5 km, 5-6 km and 6-7 km to cover different geological conditions. The "geothermal atlas" of Germany (Schulz et al. 2013) provides the map of the fault zones (Fig. 1) and information about the total length of fault zones in the four regions. A representative result of the geothermal potential utilizable for electricity production from deep rooting fault zones in Germany is about $7.7 \cdot 10^{20}$ J or $7.78 \cdot 10^{20}$ J for 20 or 50 m broad fault zones (Kuder 2018).

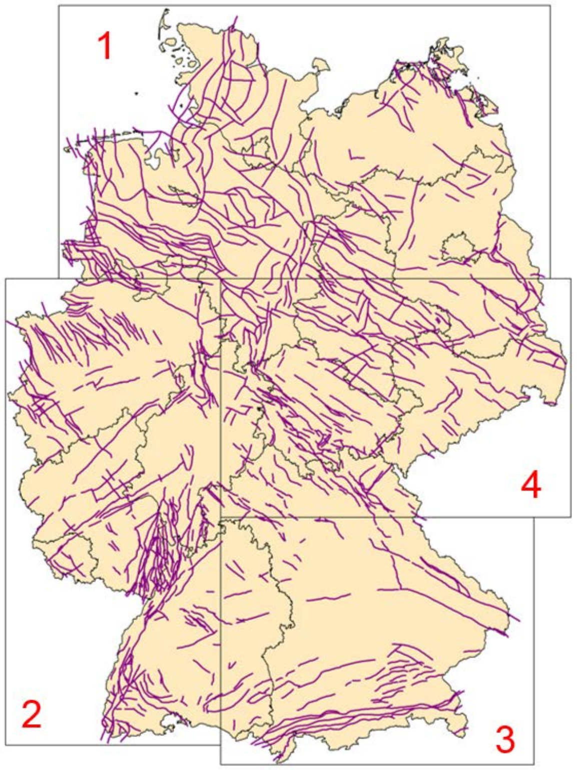

Figure 1: German fault zones, segmentation in 4 regions, length of fault systems: 7687 km North Germany (1), 7337 km West Germany (2), 2989 km South Germany (3), 6338 km Central Germany (4).

2. UNIFIED NUMERICAL MODEL

The fault systems in the numerical model are reduced to simplified fractured zones acting as black boxes with parameters representing the entire system, Fig. 2.

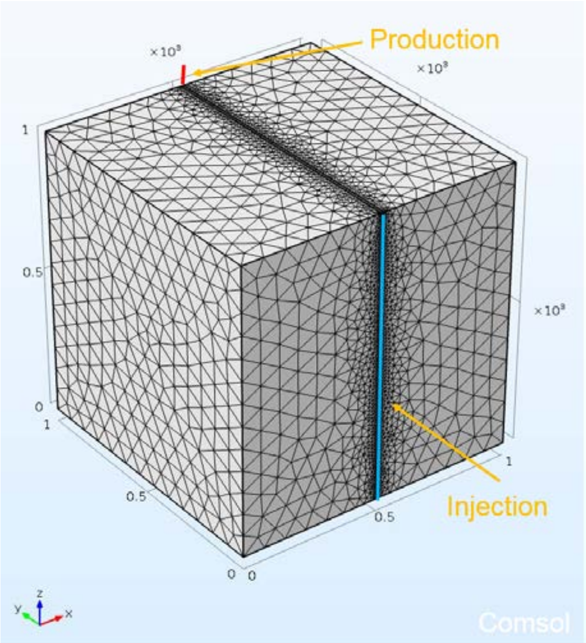

Figure 2: Unified numerical model: dimensions of model 10^9 m^3, injection and production well 1000 m, 1000 m fault zone length and 20 m or 50 m width, injection temperature 70 °C.

In total, 919 generalized fault systems are used with a length of 24351 km in contrast to 20000 km of the assessment in the study of Jung et al. (2002). The fault zones are assigned to four representative regions of Germany (Fig. 1) to allow a finer setting of the properties of the numerical models, mainly for porosity and permeability parametrisation of the rocks and faults. The total length of the fault zones in the regions are respectively: 7687 km in North Germany or region (1), 7337 km in West Germany or region (2), 2989 km in South Germany or region (3) and 6338 km in Central Germany or region (4). An internal GeotIS-database provides the porosity and permeability data obtained from core samples. Unfortunately, there is no distinctive information if the core samples are extracted from fault zones or surrounding rocks. Therefore, the approach to obtain porosity and permeability data was to assign the percentile 25 of all data in the corresponding depth interval and region as the average porosity or permeability of the surrounding rock and the percentile 95 as the average value of the fault zone. The percentiles are selected because of the following assumptions: High porosity and permeability values are indications of probed fault zones. The unified numerical model represents a fault zone and surrounding rocks with average homogenous properties, like a black box, (Fig. 2). Hence, the chosen values are the average or effective values of the real but unknown values of the complex geology. The values of the chosen percentiles are in good correlation with the permeability and porosity values of the host rocks and fault zones compared to e.g. Agosta et al. (2007) and Moeck (2014). In Western Germany (region 2) for example, there are no permeability and porosity data beneath 4 km. In this situation, the values of the previous depth interval, 3-4 km, are used for the deeper lying intervals (Table 1).

Table 1: Data of core samples provided by the Geothermal Information System (GeotIS) database. Host rock data are the percentile 25 and fault zone data are the percentile 95 of the porosity (Poro) and permeability (Perm) data. The permeability data are in milliDarcy (mD) and the values of the porosity data are normalised to 1.0.

Region 1 North Germany				
Depth	Host Rock		Fault Zone	
(km)	Perm (mD)	Poro	Perm (mD)	Poro
3-4	0.0289	0.018	28.5	0.22
4-5	0.02	0.022	21.7	0.152
5-6	0.017	0.027	21	0.144
6-7	0.001	0.005	0.56	0.05
Region 2 West Germany				
Depth	Host Rock		Fault Zone	
(km)	Perm (mD)	Poro	Perm (mD)	Poro
3-4	0.01	0.014	0.46	0.124
4-5	0.01	0.014	0.46	0.124
5-6	0.01	0.014	0.46	0.124
6-7	0.01	0.014	0.46	0.124
Region 3 South Germany				
Depth	Host Rock		Fault Zone	
(km)	Perm (mD)	Poro	Perm (mD)	Poro
3-4	0.009	0.017	710	0.172
4-5	0.085	0.026	64	0.135
5-6	0.085	0.026	64	0.135
6-7	0.085	0.026	64	0.135
Region 4 Central Germany				
Depth	Host Rock		Fault Zone	
(km)	Perm (mD)	Poro	Perm (mD)	Poro
3-4	0.011	0.019	35	0.134
4-5	0.0121	0.029	5.2	0.117
5-6	0.0121	0.029	5.2	0.117
6-7	0.0121	0.029	5.2	0.117

The fluid and rock properties of fault zones are modelled with simplifications and assumptions (Kuder 2018). The first assumption is that in the initial state the pore pressure and the fluid column in the injection well is in equilibrium. The only considered substance in the fluid beside water is NaCl with assumed concentrations of 0, 130 or 283 kg NaCl per 1 m^3, related to a low, an average or a high salinization level. Other fluid contents, like $CaCl_2$, are neglected because of the mass dominance of NaCl in the fluid and to simplify the computations (Rowe and Chou 1970). The initial pressure in the fluid column and the density of the fluid were calculated iteratively because of the dependencies on pressure, density and temperature. In the initial state, the depth is directly related to the temperature because of use of the geothermal gradient. For each concentration five fit curves are constructed for implementation in COMSOL® to describe the initial pressure, the density, the viscosity, the specific heat capacity and the thermal conduction of the fluids. The fit curves enables COMSOL® to calculate the fluid density as a function of the temperature during the fluid injection, but without considering the pumping pressure which is needed to inject the fluid. The difference between initial and pressure during injection depends on the mass of the injected fluid, the porosity and permeability of the fault zone and the host rock.

The discrepancies are not considered because of the small influence of the pressure on the density in contrast to the temperature, and to simplify the numerical simulation. This is also valid for the fluid thermal conductivity, the fluid specific heat capacity and fluid viscosity. The data points of the thermal conductivity and specific heat capacity of a fluid containing NaCl are extracted from the data tables of Phillips et al. (1981) with regard to the temperature and the initial pressure. The viscosity is calculated with the equations provided by Meehan (1980) depending on the pressure, the temperature and the content of NaCl in the fluid. Only three rock properties were applied in the numerical models with a low, an average and a high value to cover the range of the density, the specific heat capacity and the thermal conductivity. With following values: density: 2200, 2700 and 3000 kg/m3, specific heat capacity: 700, 900 and 1100 J/kg·K, thermal conduction: 1, 2.5 and 5 W/m·K. The comparison with data in Czermak et al. (1982) and Eppelbaum et al. (2014) point out that the selected values of the rock properties are reliable and representative values. The basic idea is to calculate every possible combination of fluid and rock properties. This increases the likelihood that a computed geothermal potential coefficient describes the individual geological situation in general.

3. RESULTS OF THE ASSESSMENT OF THE GEOTHERMAL POTENTIAL

The assessment of the geothermal potential of fault zones in Germany for power production is straightforward and the following calculation is just one possible example of many others (Kuder 2018). It is carried out for 20 m and 50 m wide fault zones. The basic concept is the computation of theoretical extractable geothermal energy utilizable to generate electricity per square kilometre fault area represented by the unified models. The used parameter sets of the models are selected regarding the location and depth of the unified model cubes in the German faulting zones. Because of the precondition of 50 years of production and to simplify the calculations, the content of NaCl is set to 130 kg per 1 m^3 fluid and the fluid flow is set to 15 kg/s. In comparison, geothermal doublet systems in Germany starts with flow rates of about 50 kg/s. In relation to the area of the used fault zone of the doublet, for example 4 square kilometre, the flow rate would be 12.5 kg/s per sq. km. The salt content is too high for South Germany but it is the only way to reach a production lifetime of 50 years at 3-4 km depth for the 20 m wide fault zone. The degree of salinity reduces the specific heat capacity of the fluid and in combination with the low fluid flow per sq. km; so it is ensured that the temperature of the extracted fluid is always above 100 °C. The assumed constraint for electricity generation. A higher thermal conduction value could also increase the lifetime to 50 years. The following boundary conditions are always applied: The input and output fluid flows are equal and were injected and produced homogenously distributed along line elements, representing the injection and production well. All outer boundaries are no flow boundaries. The model temperatures are calculated with the geothermal gradient 30 °C/km + 10 °C surface temperature. The injection temperature depends after Jung et al. (2002) on the type of use of the geothermal energy: power-heat coupling with heat pump: 30 °C, power-heat coupling without heat pump: 50 °C and electric power generation: 70 °C. The time step of the model calculations is 1 year. The calculations are carried out without gravity effects (Bächler et al. 2003), because the differences of the obtained geothermal energy of random sample models with and without gravity effects is only 0.1 - 1%. The low impact of the gravity is probably caused by the averaging effect of the calculation method of the geothermal energy.

Table 2: Coefficients of calculated Potential Geothermal Energy for 20 m wide fault zones

Region 1 North Germany			
Depth	Coefficient	Energy Faults	Rock Parameter
(km)	(PetaJoule)	(PetaJoule)	(see text)
3-4	3.6	27673.2	1
4-5	6.5	49965.5	2
5-6	9.16	70412.92	3
6-7	12.17	93550.79	4
Region 2 West Germany			
Depth	Coefficient	Energy Faults	Rock Parameter
(km)	(PetaJoule)	(PetaJoule)	(see text)
3-4	3.9	28614.3	1
4-5	6.59	48350,83	2
5-6	9.33	68454.21	3
6-7	12.17	89291.29	4
Region 3 South Germany			
Depth	Coefficient	Energy Faults	Rock Parameter
(km)	(PetaJoule)	(PetaJoule)	(see text)
3-4	3.57	10670.73	1
4-5	6.43	19219.27	2
5-6	9.22	27558.58	3
6-7	12.16	36346.24	4
Region 4 Central Germany			
Depth	Coefficient	Energy Faults	Rock Parameter
(km)	(PetaJoule)	(PetaJoule)	(see text)
3-4	3.58	22690.04	1
4-5	6.52	41323.76	2
5-6	9.24	58563.12	3
6-7	12.16	77070.08	4

The selected geothermal coefficients, to assess the total utilizable geothermal energy potential, are multiplied with the fault zone lengths of the corresponding regions for each depth interval and added up. Table 2, as an example, lists the used geothermal coefficients and the energy values of 20 m wide fault systems of each region and depth interval. The data for 50 m wide fault systems is be found in Kuder (2018). The total length of the fault zones in the regions are respectively: 7687 km in North Germany, 7337 km in West Germany, 2989 km in South Germany and 6338 km in Central Germany. The rock parameters used for all regions are:

(1) Depth 3–4 km: density 2200 kg/m^3, specific heat capacity 700 J/(kg·K), thermal conduction 1 W/(m·K)

(2) Depth 4–5 km: density 2700 kg/m^3, specific heat capacity 900 J/(kg·K), thermal conduction 1 W/(m·K) (fig. 13)

(3) Depth 5–6 km: density 2700 kg/m^3, specific heat capacity 700 J/(kg·K), thermal conduction 2.5 W/(m·K)

(4) Depth 6–7 km: density 3000 kg/m^3, specific heat capacity 900 J/(kg·K), thermal conduction 5 W/(m·K).

Under these conditions the total utilizable geothermal energy potential for 50 years for power production is $7.7 \cdot 10^{20}$ J for 20 m wide fault zones and $7.78 \cdot 10^{20}$ J for 50 m wide fault zones.

The quantity of electricity that could be generated from this potential depends on the energy losses during the transport to the surface and the effectivity of the conversion technology. The difference between both calculated energy potentials is only about 1% and therefore in the range of error. The thermal energy transport capability of 15 kg/s fluid is accountable for the equal results. At certain depths, even rocks with low specific heat capacity and thermal conductivity contain more thermal energy than 15 kg/s fluid can extinct in 50 years. Only at the depth of 3-4 km, there is sometimes not enough energy for fluids without NaCl. A larger quantity of NaCl in the fluid reduces the specific heat capacity depending on the temperature. In some cases that is an advantage because then host rocks in relatively low depth are not cooled down so fast and the lifetime can reach 50 years. In rocks with higher temperatures, it could be a disadvantage, because then the production rate is lower. At higher fluid flows (≥60 kg/s), the value of thermal conduction and specific heat capacity of the surrounding rocks affect apparently the magnitude of the geothermal potential.

Comparison of the results for the 20 m and 50 m wide fault zones (Fig. 3 and Fig. 4) shows that the width of the fault zones influence the geothermal potential growth depending on the watered heat exchanging space. If the permeability of the 20 m wide fault zone is small, the fluid migrate possibly into the surrounding rocks, expanding the heat exchanging space and the available geothermal energy potential. Regarding the constraint that the injected fluid mass is equal to the produced fluid mass. In case of the 50 m wide fault zone with the same conditions, it is possible that the fluid did not migrate as strong into the host rock, because it is drained by the fault zone and the heat exchange space is smaller. Consequently, the available geothermal energy potential is smaller

3. CONCLUSIONS

The geothermal potential of deep rooting fault zones was numerical modelled assisted by a generalized model to estimate the electric power production for a lifetime of 50 years with the condition that fluid temperatures are equal or greater than 100 °C. A cube with 1 km side length served as unified numerical model including a 20 or 50 meter broad, 1000 m high and 1000 m long fault zone.

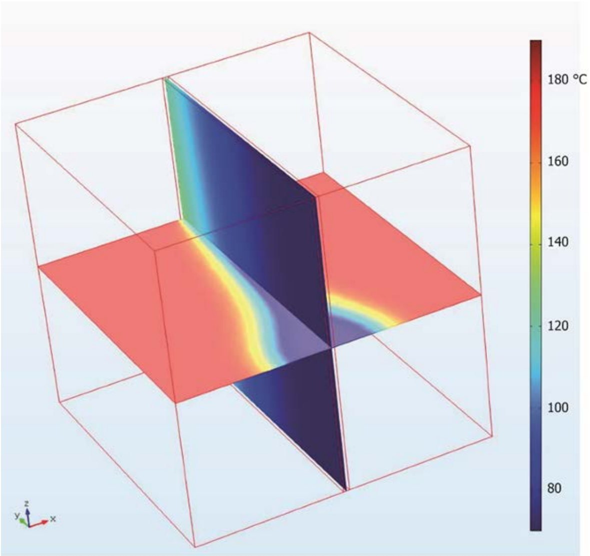

Figure 3: Temperature distribution in computed model in West Germany: depth: 5-6 km, fault zone width: 20 m, fluid flow: 60 kg/s, NaCl per m^3: 130 kg, rock: density: 2700 kg/m^3, specific heat capacity: 700 J/(kg·K), thermal conductivity: 2.5 W/(m·K), production years: 50, total energy: $2.838 \cdot 10^{16}$ Joule per 1000 m fault length.

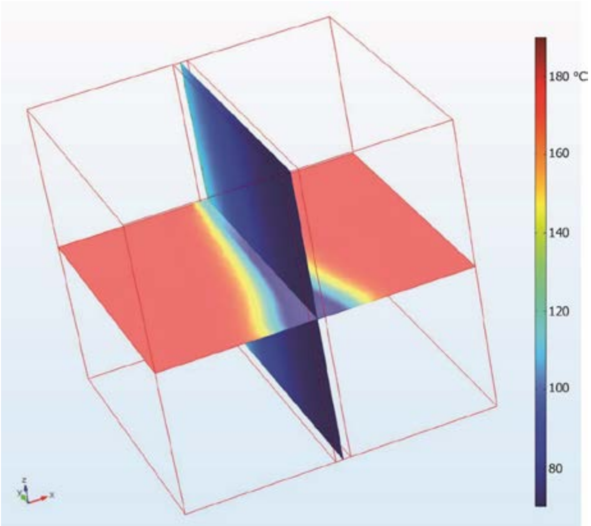

Figure 4: Temperature distribution in computed model in West Germany: depth: 5-6 km, fault zone width: 50 m, fluid flow: 60 kg/s, NaCl per m^3: 130 kg, rock: density: 2700 kg/m^3, specific heat capacity: 700 J/(kg·K), thermal conductivity: 2.5 W/(m·K), production years: 50, total energy: $2.773 \cdot 10^{16}$ Joule per 1000 m fault length.

The models were calculated with a variety of fluid and rock property parameters for four representative regions in Germany and depth ranges of 3-4 km, 4-5 km, 5-6 km and 6-7 km to cover different geological conditions. The temperature field was calculated with the average geothermal gradient in Germany. The computed coefficients for potential geothermal energy (Kuder 2018) allow a quick assessment of the utilizable geothermal potential of a fault zone to produce electricity. In addition the results show, that the geothermal potential of fault zones of varying extend can be assessed with the calculated coefficients of the unified models with a magnitude of error depending on rock temperature, the height of the fault system and the ratio of flow rate to km^2.

REFERENCES

Agosta, F., Prasad, M. and Aydin, A.: Physical properties of carbonate fault rocks, fucino basin (Central Italy): implications for fault seal in platform carbonates. *Geofluids*, **7**, (2007), 19-32.

Bächler, D., Kohl, T. and Rybach, L.: Impact of graben-parallel faults on hydrothermal convection - Rhine Graben case study; *Physics and Chemistry of the Earth*, **28**, (2003), 431 –441.

Czermak, V., Huckenholz, H. G., Rybach, L., Schmid, R., Schopper, J. R., Schuch, M., Stöffler, D. and Wohlenberg, J.: Zahlenwerte und Funktionen aus Naturwissenschaften und Technik, Neue Serie, Gruppe V: Geophysik und Weltraumforschung, Band 1, Physikalische Eigenschaften der Gesteine, Teilband a, *Springer-Verlag* Berlin, (1982).

Economides, M. and Ungemach, P. (Eds.): Applied Geothermics. *John Wiley & Sons*, (1987).

Eppelbaum, L., Kutasov, I. and Pilchin, A.: Thermal Properties of Rocks and Density of Fluids. Applied Geothermics. *Heidelberg, Springer-Verlag* Berlin, (2014).

Gringarten, A. C.; Witherspoon, P. A. and Ohnishi, Y.: Theory of Heat Extraction From Fractured Hot Dry Rock, *Journal of Geophysical Research*, Vol. **80**, No. 8, (1975), 1120 – 1124.

Gringarten, A. C.: Reservoir Lifetime and Heat Recovery Factor in Geothermal Aquifers Used for Urban Heating. *Pure and Applied Physics*. **117**, (1987), 297-308.

Haenel, R and Staroste, E. (Eds.): Atlas of Geothermal Ressorces in the European Community, Austria and Switzerland. - Publ. No. EUR 17811 of the European Commission, 92 S., *Office of Official Publications of the European Communities*, Luxemburg, (1988).

Horne, R. N.: Geothermal Energy Assessments. Geothermal Reservoir Engineering, *Kluwer Academic Publ.*, (1988), 7-21.

Jain, C., Vogt, C. and Clauser, C.: Maximum potential for geothermal power in Germany based on engineered geothermal systems. *Geothermal Energy*, **3** (1), (2015), 15.

Jung, R., Röhling, S., Ochmann, N., Rogge, S., Schellschmidt, R., Schulz, R., Thielemann, T. (2002): Abschätzung des technischen Potenzials der geothermischen Stromerzeugung und der geothermischen Kraft-Wärme-Kopplung (KWK) in Deutschland. *BGR*, Hannover, (2002).

Kuder, J.: Assessment of the Geothermal Potential of Fault Zones in Germany by Numerical Modelling. *ZDGG*, (2018), DOI:10.1127/zdgg/2018/0130.

Meehan, D. N.: A Correlation For Water Viscosity. *Petroleum Engineer International*, July 1980.

Moeck, I.S.: Catalog of geothermal play types based on geologic controls. *Renewable and sustainable energy reviews*, **37**, (2014), 867–882.

Muffler, P. and Cataldi, R.: Methods for regional assessment of geothermal resources, *Geothermics*, **7**, (1978), 53-89.

Nathenson, M.: Physical factors determining the fraction of stored energy recoverable from hydrothermal convection systems and conduction dominated areas. – In: *U.S. Geol. Survey Open-File Report*, (1975), 75–525: 38 p.

Phillips, S. L., Igbene, I., Fair, J. A.; Ozbeck, H. and Tavana, M.: A Technical Databook for Geothermal Energy Utilization. *Lawrence Berkeley Laboratory, University of California*, LBL-12810, Berkley, (1981).

Rowe, A and Chou, J.: Pressure-Volume-Temperature-Concentration Relation of Aqueous NaCl Solutions. *Journal of Chemical and Engineering Data*, Vol. **15**, No. 1, (1970), 61-66.

Rühaak, W., Rath, V. and Clauser, C.: Detecting thermal anomalies within the Molasse Basin, Southern Germany. *Hydrogeology Journal* **18(8)**: (2010), 1897-1915.

Schulz, R., Suchi, E., Öhlschläger, D., Dittmann, J., Knopf, S. and Müller, C.: Geothermie-Atlas zur Darstellung möglicher Nutzungskonkurrenzen zwischen CCS und Tiefer Geothermie. Endbericht, Archiv-Nr. 131 310, 108, *LIAG*, Hannover, (2013).

Acknowledgements

The numerical models were developed with the simulation software COMSOL Multiphysics® a finite element analysis, solver and simulation software package for various physics and engineering applications. The Federal Ministry for Economic Affairs and Energy supported this in the framework of the joint project “Die Rolle von tiefreichenden Stör-ungszonen bei der geothermischen Energienutzung”, No.: 0325623A.